Accepted Manuscript

Patient-specific estimates of vascular and placental properties in growth-restricted fetuses based on a model of the fetal circulation

Patricia Garcia-Canadilla, PhD, Fatima Crispi, MD, Monica Cruz-Lemini, MD, Stefania Triunfo, MD, Alfons Nadal, MD, Brenda Valenzuela-Alcaraz, MD, Paula A. Rudenick, PhD, Eduard Gratacos, MD, Bart H. Bijnens, PhD

PII: S0143-4004(15)30024-2

DOI: 10.1016/j.placenta.2015.07.130

Reference: YPLAC 3243

To appear in: *Placenta*

Received Date: 4 June 2015

Revised Date: 21 July 2015

Accepted Date: 22 July 2015

Please cite this article as: Garcia-Canadilla P, Crispi F, Cruz-Lemini M, Triunfo S, Nadal A, Valenzuela-Alcaraz B, Rudenick PA, Gratacos E, Bijnens BH, Patient-specific estimates of vascular and placental properties in growth-restricted fetuses based on a model of the fetal circulation, *Placenta* (2015), doi: 10.1016/j.placenta.2015.07.130.

Patient-specific estimates of vascular and placental properties in growth-restricted fetuses based on a model of the fetal circulation

Patricia GARCIA-CANADILLA, PhD,[1,2] Fatima CRISPI, MD,[1,3] Monica CRUZ-LEMINI, MD,[1] Stefania TRIUNFO, MD,[1] Alfons NADAL, MD,[4] Brenda VALENZUELA-ALCARAZ, MD[1] Paula A. RUDENICK, PhD,[2] Eduard GRATACOS, MD,[1,3] and Bart H. BIJNENS, PhD.[2,5]

[1] Fetal i+D Fetal Medicine Research Center, BCNatal - Barcelona Center for Maternal-Fetal and Neonatal Medicine (Hospital Clínic and Hospital Sant Joan de Deu), IDIBAPS, University of Barcelona, Spain.

[2] Physense, DTIC, Universitat Pompeu Fabra, Barcelona, Spain.

[3] Centre for Biomedical Research on Rare Diseases (CIBER-ER), Spain.

[4] Department of Pathology, Hospital Clinic – IDIBAPS, University of Barcelona, Barcelona, Spain

[5] ICREA, Barcelona, Spain.

Conflict of interest: The authors report no conflict of interest.

This study was partly supported by grants from Ministerio de Economia y Competitividad (ref. SAF2012-37196); the Instituto de Salud Carlos III (ref. (PI11/01709, PI12/00801, PI14/00226) integrado en el Plan Nacional de I+D+I y cofinanciado por el ISCIII-Subdirección General de Evaluación y el Fondo Europeo de Desarrollo Regional (FEDER) “Otra manera de hacer Europa”; the EU FP7 for research, technological development and demonstration under grant agreement VP2HF

(no 611823); The Cerebra Foundation for the Brain Injured Child (Carmarthen, Wales, UK); Obra Social “la Caixa” (Barcelona, Spain); P.G.C. was supported by the Programa de Ayudas Predoctorales de Formación en investigación en Salud (FI12/00362) from the Instituto Carlos III, Spain;. M.C.L. and B.V.A. wish to express their gratitude to the Mexican National Council for Science and Technology (CONACyT, Mexico City, Mexico) for supporting their predoctoral stay at Hospital Clinic, Barcelona, Spain.

Address correspondence to: Patricia Garcia-Canadilla, Fetal i+D Fetal Medicine Research Center, BCNatal - Barcelona Center for Maternal-Fetal and Neonatal Medicine, Sabino de Arana 1, 08028, Barcelona, Spain.

Name: Patricia Garcia-Canadilla

Phone: +34932279946 or +34932279906.

Fax: +34932275605

E-mail: patricia.garciac@upf.edu

ABSTRACT

INTRODUCTION: Intrauterine growth restriction (IUGR) due to placental insufficiency is associated with blood-flow redistribution in order to maintain perfusion to the brain. However, some hemodynamic parameters that might be more directly related to staging of the disease cannot be measured non-invasively in clinical practice. For this, we developed a patient-specific model of the fetal circulation to estimate vascular properties of each individual.

METHODS: A lumped model of the fetal circulation was developed and personalized using measured echographic data from 37 normal and IUGR fetuses to automatically estimate model-based parameters. A multivariate regression analysis was performed to evaluate the association between the Doppler pulsatility indices (PI) and the model-based parameters. The correlation between model-based parameters and the placental lesions was analyzed in a set of 13 IUGR placentas. A logistic regression analysis was done to assess the added value of the model-based parameters relative to Doppler indices, for the detection of fetuses with adverse perinatal outcome.

RESULTS: The estimated model-based placental and brain resistances were respectively increased and reduced in IUGR fetuses while placental compliance was increased in IUGR fetus. Umbilical and middle cerebral arteries PIs were most associated with both placental resistance and compliance, while uterine artery PI was more associated with the placental compliance. The logistic regression analysis showed that the model added significant information to the traditional analysis of Doppler waveforms for predicting adverse outcome in IUGR.

DISCUSSION: The proposed patient-specific computational model seems to be a good approach to assess hemodynamic parameters than cannot be measured clinically.

KEYWORDS: computational model; fetal circulation; Doppler; placental resistance

1. Introduction

Intrauterine growth restriction (IUGR) from placental insufficiency is one of the leading causes of perinatal mortality/morbidity [1,2]. It is associated with blood-flow redistribution that involves several vessels of the feto-placental circulation, such as the aortic isthmus (AoI), middle cerebral artery (MCA) and the umbilical artery (UA). This blood-flow redistribution due to IUGR is thought to be caused by the increase in the placental and peripheral resistances and the decrease of brain resistance due to cerebral arteries vasodilation, and is associated with worse perinatal, neurodevelopmental and cardiovascular outcome [3–7]. In clinical practice, these fetal hemodynamic changes are evaluated by quantifying the Doppler flow-velocity waveforms using empirical pulsatility indices (PI). However, in some small for gestational age (SGA) fetuses, placental histological changes compatible with placental under-perfusion, defined as any maternal and/or fetal vascular pathology, were identified without changes in the Doppler indices [8,9]. Moreover, signs of placental under-perfusion have been associated with an increased risk of neonatal morbitidy [10,11] and abnormal neurodevelopmental outcome [8].

It is commonly believed that an increase in the pulsatility of the arterial flow is caused by an increase in vascular resistance. Several studies in an IUGR sheep model [12–16], or using an electrical-analog model of the placental circulation [14,16–19], have evaluated the association between different alterations in vascular structures and beds with the Doppler in the UA and uterine artery (UtA). These studies supported that the UA–PI is directly related to high placental and low UA resistance or a combination of high placental resistance and UA wall abnormalities. However, in other studies, using vasoactive agents to increase resistance, a poor correlation between pulsatility and resistance was found. In the UtA, similarly to the UA, some fetal sheep studies [15]

demonstrated that when the placental microcirculation was occluded, resistance was increased and abnormal Doppler waveforms were observed. However, UtA Doppler is also influenced by maternal factors [20], and therefore abnormal patterns could not be explained only by the changes in placental vasculature. Thus, there are several hemodynamic factors that can lead to abnormal Doppler waveforms in both UA and UtA, and not all changes originate from an increase in placental resistance.

All theses studies were performed in animal models or using electrical equivalent models. However, it is not feasible to study, in-vivo and non-invasively, the underlying hemodynamic determinants of the Doppler-waveforms in different vessels in human fetuses and alternative approaches need to be used. To better understand hemodynamic remodeling, a patient-specific model of the fetal circulation can be used to estimate different vascular and hemodynamics properties of each patient that cannot be assessed during the ultrasonography evaluation. Despite that several models of the fetal circulation have been developed, only few of them were patient-specific [21,22]. Our purpose was to use a lumped model of the fetal circulation to estimate patient-specific vascular and placental properties of normal and IUGR fetuses. This might help in the understanding of IUGR and its underlying mechanisms and to compare the diagnostic performance of those variables for prediction of increased risk of adverse perinatal outcome.

2. Methods

2.1 Study population

Ultrasonographic data from IUGR and normally grown fetuses (controls) were used to fit the computational model. IUGR and control fetuses were selected from singleton pregnancies who attended for routine hospital visit in the third trimester of pregnancy at the Maternal-Fetal Medicine Department at BCNatal in Barcelona between January 2010 and April 2014. Eighty percent of the fetuses included were already included in previous studies from our group [23,24]. IUGR was defined as an estimated fetal weight (EFW) and confirmed birth weight below the 10^{th} centile according to local reference curves [25] together with a pulsatility index (PI) in the UA above 2 standard deviations [26]. Controls were selected among non-complicated pregnancies with EFW and birthweight above 10^{th} centile [25]. Pregnancies with structural/chromosomal anomalies or evidence of infection were excluded. The study protocol was approved by the local Ethics Committee and parents provided written informed consent.

In all fetuses, biometrics and feto-placental Doppler, including flow velocities in the UA, UtA, MCA, AoI and right and left ventricle (RV and LV) outflow tracks were performed using a Siemens Sonoline Antares (Siemens Medical Systems, Malvern, PA, USA). Details on the ultrasonographic evaluation can be found in the Supplementary Methods.

At delivery, gestational age (GA), birth weight, birth weight centile, mode of delivery, Apgar scores, umbilical pH, presence of preeclampsia and length of stay at the neonatal intensive care unit were also recorded. Adverse perinatal outcome was defined as the presence of at least one of the following: umbilical artery pH<7.15, 5-min APGAR score <7.0, admission to neonatal care unit for a period of at least 25 days or intervention for fetal distress.

2.2 Patient-specific modeling

2.2.1 Lumped model of the fetal circulation

An improved version of our previous model of the fetal circulation [22] was implemented. New arterial segments and vascular beds of the downstream fetal circulation were included. Specifically, the descending aorta was replaced by the thoracic and abdominal aorta, two iliac and two UA. The peripheral vascular bed was replaced by two kidneys, two lower body and placental vascular beds. The model consisted of 19 arterial segments and 12 vascular beds as shown in Figure 1.

As described in Garcia-Canadilla et al [22], the equivalent lumped model was constructed by interconnecting two different building blocks: (1) the arterial segment, which included a capacitor (C), a resistor (R) and an inductor (L), representing arterial compliance, resistance of blood flowing in the arterial segment and blood inertia respectively; and (2) the vascular bed, consisting of a three-element Windkessel model, which included a resistor and a capacitor representing the vascular bed resistance and compliance respectively. The equivalent lumped model of the fetal circulation consists of a total of 94 electrical components and 2 inputs, and was implemented in MATLAB (2013b, The MathWorks Inc., Natick, MA).

2.2.2 Patient-specific input data

Patient-specific blood velocity waveforms from RV and LV outflow tracks (V_{RV} and V_{LV}), AoI (V_{AoI}), MCA (V_{MCA}) and UA (V_{UA}) were obtained by manual delineation of the envelope of the respective Doppler profiles. The corresponding blood-flows: Q_{LV}, Q_{RV}, Q_{AoI} , Q_{MCA} and Q_{UA} were calculated. Details on the blood-flow calculation are described in Supplementary Methods. The GA and EFW were used to calculate the different electrical components of the equivalent circuit. The detailed description of the

calculation of the electrical components of the model is described in Supplementary Methods.

2.2.3 Patient-specific fitting

A diagram of the patient-specific fitting algorithm is shown in Figure 2. The input of the model was the set of the patient-specific nominal values of all electrical components, and two patient-specific blood-flow inputs: Q_{RV} and Q_{LV}. The output was the model-based blood velocities in the AoI ($\widetilde{V}_{AoI}$), MCA ($\widetilde{V}_{MCA}$) and UA ($\widetilde{V}_{UA}$). In order to fit the model-based blood-flows to the measured ones, an optimization algorithm was used to estimate a set of 13 model parameters. The set of parameters was estimated automatically for each patient, using a constrained nonlinear optimization algorithm minimizing the error between the model-based and measured blood velocity waveforms of the AoI, MCA and UA. Details on the optimization process can be found in Supplementary Methods.

2.3 Placental evaluation

Placental examinations adhered to standard laboratory protocol. Fresh and trimmed (after removal of the membranes, cord, and any blood clots) placental weight was recorded. Trimmed placental weight centiles were assigned based on GA-specific placental weight charts [27]. The feto-placental weight ratio (birth weight/fresh placental weight) was also expressed as a percentile, drawn from GA-specific ranges [28].

Placentas were fixed in 10% buffered formalin. After gross examination, samples of each specimen were taken for routine processing: one transverse section of cord, one rolled strip of membranes, and three blocks of villous parenchyma. All macroscopic lesions were sampled as well. Finished slides were hematoxylin and eosin-stained. A single senior pathologist (AN) supervised all examinations.

Using a hierarchical and standardized classification system, as previously described by our group [10], histologic manifestations were further designated as maternal (MUP) or fetal (FUP) in origin, defined as placental under perfusion (PUP) [29–31]. All placental evaluation was performed by the same histopathologist, blinded for the clinical and model-based data. Details on the histological placental examination are described in Supplementary Methods.

2.4 Statistical analysis

A student's t-test or Mann-Whitney U test were used to compare quantitative normally and not normally distributed data, respectively between groups. Pearson chi-square was used to compare qualitative data between groups. A multivariate regression analysis was performed to evaluate the association between Doppler indices and different hemodynamic variables. Finally, associations between different Doppler and model-based parameters and IUGR and adverse perinatal outcome were analyzed by multiple logistic regressions using SPSS 17.0.

3. Results

3.1. Study populations

A total of 48 fetuses, 21 IUGR cases and 27 controls, were initially included in the study (median GA at fetal ultrasound: 31.4 weeks; range: 27.4-38.2). Patient-specific fitting was successfully performed in 37 fetuses, including 15 IUGR cases and 22 controls, which represents a success rate of 77 %. Eleven cases could not be modeled with the current approach because of non-convergence of the fitting algorithm, predominantly due to low quality of the measured Doppler waveforms (which were not specifically acquired for the purpose of modeling). Table 1 compares the feto-placental ultrasonographic data and perinatal outcome by study group. As expected, birthweight

and GA at delivery were significantly lower in IUGR with worse feto-placental Doppler and perinatal outcome.

3.2. Model-based parameters and feto-placental Doppler

Figure 3 shows the measured and model-based velocity waveforms in the AoI, MCA and UA for a control (3a-3f) and IUGR fetus (3g-3l). Table 2 shows the model-based parameters obtained for both groups after the minimization process. The estimated placental resistance and compliance were significantly increased in IUGR. On the other hand, coronary arteries and brain resistances were significantly lower. There were no significant differences in the other 11 estimated model-based parameters.

Table 3 shows the association between Doppler and model-based parameters by means of multivariate regression. While UA-PI, MCA-PI and CPR showed a significant association with both model-based placental resistance and compliance, UtA-PI was only significantly associated with the model-based placental compliance. AoI was significantly associated to coronary arteries resistance.

3.3. Model-based parameters and placental evaluation

Histological evaluation was performed in 13 of the 15 IUGR placentas. In a total of 13 IUGR placentas, 13 PUP-related histopathology was identified in 8 cases (Table 4). Placental weight mean was 313.8gr (± 88.71) and fetoplacental weight ratio 4.69 (± 1.30) respectively.

Figure 4 shows the model-based parameters for the 13 placentas histologically evaluated, classified in three different groups according to the PUP-related histopathology: normal (n=5), MUP (n=5) and MUP & FUP (n=3). The K_{Rplac} and K_{Cplac} model-based parameters were transformed to $1/K_{Rplac}$ and $1/K_{Cplac}$ to have a normal distribution. Although the differences between groups were not statistically significant, those placentas with signs of MUP as well as FUP showed a linear tendency to have

decrease values of both $1/K_{Rplac}$ and $1/K_{Cplac}$. However, the placentas with only signs of MUP showed a linear tendency to have a decrease in $1/K_{Rplac}$ and not in $1/K_{Cplac.}$ Finally, both PUP groups showed a linear tendency to have a decrease in K_{RcorA}.

3.4. Model-based parameters and perinatal outcome

The results of the logistic regression analysis showed that with model-based parameters, the accuracy, sensitivity and specificity of detecting IUGR fetus was 100%.

Next, the fetal population was classified to have or not have adverse perinatal outcome. Table 5 shows the main perinatal data, Doppler parameters before delivery and the model-based parameters for both groups. Again, GA at delivery and birth-weight were significantly lower in those fetuses that had adverse perinatal outcome. Model-based placental resistance and compliance were significantly higher and brain and coronary arteries resistances were significantly lower in fetuses with poorer perinatal outcome. Figure 5 shows the four model-based parameters that were significantly different between the different groups: controls, IUGR and fetuses with adverse perinatal outcome. Table 6 shows the results from the logistic regression performed with different sets of Doppler and model-based parameters. Using the Doppler parameters alone, the sensitivity was 72.7%. On the other hand, GA alone showed a better predictive capacity than Doppler parameters, with a sensitivity of 81.8%. When the estimated model-based parameters were included, the detection of adverse perinatal outcome was considerably improved up to a sensitivity of 90.9%.

Discussion

We presented a lumped model of the fetal circulation for estimating patient-specific vascular and placental properties. The model was successfully used for evaluating a cohort of 37 control and IUGR fetuses. The results shown that UA and MCA PIs were most associated with both placental resistance and compliance, while UtA-PI was more

associated with the placental compliance. Also we demonstrated that adding the model-based parameters to the conventional Doppler parameters improve the detection of fetuses with adverse perinatal outcome.

Several computational models [18,21,22,32–35] have been developed and used to improve the understanding of the Doppler changes observed in IUGR at different locations in the fetal circulation, such as UA and UtA. However only few [21,22] were patient-specific and allow estimation of an individual set of hemodynamic parameters. Our extended lumped model was used to estimate a set of thirteen vascular parameters in a cohort of 22 controls and 15 IUGR fetuses. From this set of estimated parameters, only four were significantly different between groups: placental resistance and compliance were higher and brain and coronary arteries resistances were lower in IUGR fetuses compared to controls. We have shown that while UA-PI, MCA-PI and CPR showed a significant association with both model-based placental resistance and compliance, UtA-PI was only significantly associated with the model-based placenta compliance. This suggests that different Doppler parameters are describing different placental substrates. While UA and MCA most probably reflect an initially abnormal placenta with less developed vasculature (reflected by increased placental resistance), UtA most probably reflects the maternal-fetal interaction that determines placental compliance.

Placental insufficiency can be caused by different patterns of placental changes, such as villious infarcts, villious fibrosis, villous hypovascularity, etc [36,37]. In fact, when we evaluated the correlation between the model-based parameters and the maternal and/or fetal signs of placental under-perfusion we found that placental compliance showed a tendency to increase only in those cases with both fetal and maternal under-perfusion while the placental resistance showed a tendency to linearly

increase with the number of placental lesions. These results support the hypothesis that placental vascular properties' changes are different depending on the origin (maternal and/or fetal) of the lesion. However, in order to further investigate this, a more detailed model of the placenta would be needed.

We also evaluated the added value of patient-specific model-based parameters in the detection of fetuses with adverse perinatal outcome in comparison to currently used Doppler parameters. When Doppler indices were used alone, the sensitivity and specificity obtained was 72.7% and 95.8% respectively. However, the addition of a set of model-based parameters improved sensitivity for the detection of adverse perinatal outcome to 90%. In a similar study [21], in which four hemodynamic parameters were estimated by a patient-specific fitting in a cohort of 42 fetuses, the addition of these parameters to the conventional Doppler indices also improved the detection of IUGR fetuses. In our study, we used a different set of hemodynamic parameters that seems to perform better in the detection of IUGR fetuses with poorer perinatal outcome. This can be explained by the fact that our set of parameters are more directly related to the disease, placental insufficiency, than the set used by Luria et al [21], who used parameters more related to blood-flow redistribution.

We acknowledge that our current model has some limitations. Apart from the ones already mentioned in our previous published model [22] this study has some additional limitations. Firstly, a set of only a few parameters was personalized for each fetus, assuming that the rest of parameters were unchanged. This simplification was necessary to make a compromise between complexity and efficiency of the model, and to avoid overfitting of the data. Therefore the number of parameters is limited to reduce the number of possible solutions of the inverse problem as done in other patient-specific models [21]. In our case, the most relevant parameters that describe the hemodynamics

of each patient were included. We did perform the simulations with a large set of parameters by considering the individual variation of each vascular bed resistance and compliance and the results obtained were the same, suggesting that the inclusion of more parameters to fit does not add significant information but considerably increase the complexity and the computational cost. Secondly, a more complex model of the placental circulation would be required to further evaluate the specific hemodynamic changes in the placenta, and to take into account the maternal factors that can influence the fetal circulation. However, evaluation of the detailed hemodynamic properties of the feto-maternal circulation of the placenta was beyond the scope of this study. Additionally, given that, in clinical practice, pressures cannot be quantitatively assessed in fetuses, we have not validated and studied the local pressures obtained from the model. However, these are within realistic ranges as reported in experimental models. Finally, the amount of patients in the study was small. Nevertheless the results look promising to directly assess hemodynamic properties of the fetal circulation rather than using Doppler measurements and to improve the detection of fetuses with adverse perinatal outcome.

The results obtained from this study suggested that patient-specific hemodynamic parameters estimated with our computational model added significant information to the conventional Doppler indices, since they describe the underlying vascular and hemodynamic properties that can not be assessed in a clinical setting. This opens opportunities to find more easily obtainable approaches to specifically assess these hemodynamic parameters the we found to be most altered by IUGR, e.g. using an even simpler model or assess other properties of local Doppler data than currently used in clinical practice. The information and knowledge provided by the model-based parameters can thus be used complementary to conventional techniques, for the

determination of the timing for delivery as well as to personalize the treatment in IUGR pregnancies.

In conclusion, we presented a patient-specific lumped model of the fetal circulation that successfully estimated a set of fetal vascular and hemodynamic properties. Placental and coronary compliance/resistance strongly correlate with feto-placental Doppler parameters, show an association with placental maternal/fetal underperfusion, and correlate with adverse perinatal outcome in IUGR. Therefore, the proposed patient-specific computational model seems to be a good approach to assess hemodynamic and placental parameters than cannot be measured non-invasively in clinical practice.

REFERENCES

[1] Alberry M, Soothill P. Management of fetal growth restriction. Arch Dis Child Fetal Neonatal Ed 2007;92:F62–7. doi:10.1136/adc.2005.082297.

[2] Figueras F, Gratacós E. Update on the diagnosis and classification of fetal growth restriction and proposal of a stage-based management protocol. Fetal Diagn Ther 2014;36:86–98. doi:10.1159/000357592.

[3] Cruz-Lemini M, Crispi F, Van Mieghem T, Pedraza D, Cruz-Martinez R, Acosta-Rojas R, et al. Risk of perinatal death in early-onset intrauterine growth restriction according to gestational age and cardiovascular Doppler indices: a multicenter study. Fetal Diagn Ther 2012;32:116–22. doi:10.1159/000333001.

[4] Eixarch E, Meler E, Iraola a, Illa M, Crispi F, Hernandez-Andrade E, et al. Neurodevelopmental outcome in 2-year-old infants who were small-for-gestational age term fetuses with cerebral blood flow redistribution. Ultrasound Obstet Gynecol 2008;32:894–9. doi:10.1002/uog.6249.

[5] Figueras F, Cruz-Martinez R, Sanz-Cortes M, Arranz A, Illa M, Botet F, et al. Neurobehavioral outcomes in preterm, growth-restricted infants with and without prenatal advanced signs of brain-sparing. Ultrasound Obs Gynecol 2011;38:288–94. doi:10.1002/uog.9041.

[6] Fouron J-C, Gosselin J, Raboisson M-J, Lamoureux J, Tison C-A, Fouron C, et al. The relationship between an aortic isthmus blood flow velocity index and the postnatal neurodevelopmental status of fetuses with placental circulatory insufficiency. Am J Obstet Gynecol 2005;192:497–503. doi:10.1016/j.ajog.2004.08.026.

[7] Hernandez-Andrade E, Crispi F, Benavides-Serralde JA, Plasencia W, Diesel HF, Eixarch E, et al. Contribution of the myocardial performance index and aortic isthmus blood flow index to predicting mortality in preterm growth-restricted fetuses. Ultrasound Obs Gynecol 2009;34:430–6. doi:10.1002/uog.7347.

[8] Parra-Saavedra M, Crovetto F, Triunfo S, Savchev S, Peguero A, Nadal A, et al. Neurodevelopmental outcomes of near-term small-for-gestational-age infants with and without signs of placental underperfusion. Placenta 2014;35:269–74. doi:10.1016/j.placenta.2014.01.010.

[9] Parra-Saavedra M, Crovetto F, Triunfo S, Savchev S, Peguero A, Nadal A, et al. Placental findings in late-onset SGA births without Doppler signs of placental insufficiency. Placenta 2013;34:1136–41. doi:10.1016/j.placenta.2013.09.018.

[10] Parra-Saavedra M, Simeone S, Triunfo S, Crovetto F, Botet F, Nadal A, et al. Correlation between histological signs of placental underperfusion and perinatal morbidity in late-onset small-for-gestational-age fetuses. Ultrasound Obstet Gynecol 2015;45:149–55. doi:10.1002/uog.13415.

[11] Parra-Saavedra M, Crovetto F, Triunfo S, Savchev S, Peguero A, Nadal A, et al. Association of Doppler parameters with placental signs of underperfusion in late-onset small-for-gestational-age pregnancies. Ultrasound Obstet Gynecol 2014;44:330–7. doi:10.1002/uog.13358.

[12] Van Huisseling H, Hasaart TH, Muijsers GJ, de Haan J. Umbilical artery pulsatility index and placental vascular resistance during acute hypoxemia in fetal lambs. Gynecol Obstet Invest 1991;31:61–6.

[13] Adamson SL. Arterial pressure, vascular input impedance, and resistance as determinants of pulsatile blood flow in the umbilical artery. Eur J Obs Gynecol Reprod Biol 1999;84:119–25.

[14] Surat DR, Adamson SL. Downstream determinants of pulsatility of the mean velocity waveform in the umbilical artery as predicted by a computer model. Ultrasound Med Biol 1996;22:707–17.

[15] Saunders HM, Burns PN, Needleman L, Liu JB, Boston R, Wortman JA, et al. Hemodynamic factors affecting uterine artery Doppler waveform pulsatility in sheep. J Ultrasound Med 1998;17:357–68.

[16] Adamson SL, Morrow RJ, Bascom PA, Mo LY, Ritchie JW. Effect of placental resistance, arterial diameter, and blood pressure on the uterine arterial velocity waveform: a computer modeling approach. Ultrasound Med Biol 1989;15:437–42.

[17] Thompson RS, Trudinger BJ. Doppler waveform pulsatility index and resistance, pressure and flow in the umbilical placental circulation: an investigation using a mathematical model. Ultrasound Med Biol 1990;16:449–58.

[18] Van den Wijngaard JPHM, Westerhof BE, Faber DJ, Ramsay MM, Westerhof N, van Gemert MJC. Abnormal arterial flows by a distributed model of the fetal circulation. Am J Physiol Regul Integr Comp Physiol 2006;291:R1222–33. doi:10.1152/ajpregu.00212.2006.

[19] Mo LY, Bascom PA, Ritchie K, McCowan LM. A transmission line modelling approach to the interpretation of uterine Doppler waveforms. Ultrasound Med Biol 1988;14:365–76.

[20] Everett TR, Lees CC. Beyond the placental bed: placental and systemic determinants of the uterine artery Doppler waveform. Placenta 2012;33:893–901. doi:10.1016/j.placenta.2012.07.011.

[21] Luria O, Bar J, Shalev J, Kovo M, Golan A, Barnea O. Inverse Solution of the Fetal-Circulation Model Based on Ultrasound Doppler Measurements. Cardiovasc Eng Technol 2014;5:202–16. doi:10.1007/s13239-013-0153-7.

[22] Garcia-Canadilla P, Rudenick PA, Crispi F, Cruz-Lemini M, Palau G, Camara O, et al. A computational model of the fetal circulation to quantify blood redistribution in intrauterine growth restriction. PLoS Comput Biol 2014;10:e1003667. doi:10.1371/journal.pcbi.1003667.

[23] Cruz-Lemini M, Crispi F, Valenzuela-Alcaraz B, Figueras F, Gómez O, Sitges M, et al. A fetal cardiovascular score to predict infant hypertension and arterial remodeling in intrauterine growth restriction. Am J Obstet Gynecol 2014;210:552.e1–552.e22. doi:10.1016/j.ajog.2013.12.031.

[24] Iruretagoyena JI, Gonzalez-Tendero A, Garcia-Canadilla P, Amat-Roldan I, Torre I, Nadal A, et al. Cardiac dysfunction is associated with altered sarcomere ultrastructure in intrauterine growth restriction. Am J Obs Gynecol 2014;210:550.e1–7. doi:10.1016/j.ajog.2014.01.023.

[25] Figueras F, Meler E, Iraola A, Eixarch E, Coll O, Figueras J, et al. Customized birthweight standards for a Spanish population. Eur J Obs Gynecol Reprod Biol 2008;136:20–4. doi:10.1016/j.ejogrb.2006.12.015.

[26] Baschat AA, Gembruch U. The cerebroplacental Doppler ratio revisited. Ultrasound Obs Gynecol 2003;21:124–7. doi:10.1002/uog.20.

[27] Almog B, Shehata F, Aljabri S, Levin I, Shalom-Paz E, Shrim A. Placenta weight percentile curves for singleton and twins deliveries. Placenta 2011;32:58–62. doi:10.1016/j.placenta.2010.10.008.

[28] Burkhardt T, Schäffer L, Schneider C, Zimmermann R, Kurmanavicius J. Reference values for the weight of freshly delivered term placentas and for placental weight-birth weight ratios. Eur J Obstet Gynecol Reprod Biol 2006;128:248–52. doi:10.1016/j.ejogrb.2005.10.032.

[29] Redline RW, Heller D, Keating S, Kingdom J. Placental diagnostic criteria and clinical correlation--a workshop report. Placenta 2005;26 Suppl A:S114–7. doi:10.1016/j.placenta.2005.02.009.

[30] Redline RW. Placental pathology: a systematic approach with clinical correlations. Placenta 2008;29 Suppl A:S86–91. doi:10.1016/j.placenta.2007.09.003.

[31] Triunfo S, Lobmaier S, Parra-Saavedra M, Crovetto F, Peguero A, Nadal A, et al. Angiogenic factors at diagnosis of late-onset small-for-gestational age and histological placental underperfusion. Placenta 2014;35:398–403. doi:10.1016/j.placenta.2014.03.021.

[32] Rudenick P, Bijnens B, Butakoff C, Garcia-Dorado D, Evangelista A. Understanding Hemodynamics and Its Determinant Factors in Type B Aortic

Dissections Using an Equivalent Lumped Model. STACOM, Proc. Int. Conf. Med. Image Comput. Comput. Assist. Interv. LNCS vol. 7746, vol. 2, 2013, p. 375–82. doi:10.1007/978-3-642-36961-2_42.

[33] Pennati G, Bellotti M, Fumero R. Mathematical modelling of the human foetal cardiovascular system based on Doppler ultrasound data. Med Eng Phys 1997;19:327–35. doi:10.1016/s1350-4533(97)84634-6.

[34] Myers LJ, Capper WL. A transmission line model of the human foetal circulatory system. Med Eng Phys 2002;24:285–94. doi:10.1016/s1350-4533(02)00019-x.

[35] Guettouche, Guettouche A, Challier JC, Ito Y, Papapanayotou C, Cherruault Y, et al. Mathematical modeling blood circulation of the human fetal arterial. Int J Biomed Comput 1992;31:127–39.

[36] Zhang S, Regnault TRH, Barker PL, Botting KJ, McMillen IC, McMillan CM, et al. Placental adaptations in growth restriction. Nutrients 2015;7:360–89. doi:10.3390/nu7010360.

[37] Madazli R, Somunkiran A, Calay Z, Ilvan S, Aksu MF. Histomorphology of the placenta and the placental bed of growth restricted foetuses and correlation with the Doppler velocimetries of the uterine and umbilical arteries. Placenta 2003;24:510–6.

TABLES

Table 1. Doppler parameters before delivery and perinatal characteristics of normally grown (control) and IUGR fetuses.

	Control (n = 22)	*IUGR (n=15)*	*p**
Feto-placental ultrasound			
AoI-PI (Z-Score)	-0.32 ± 0.74	18.39 ± 29.77	0.005
IFI (Z-Score)	0.49 ± 0.87	-5.59 ± 7.50	0.001
MCA-PI (Z-score)	0.27 ± 0.96	-1.26 ± 0.95	<0.001
UA-PI (Z-score)	-0.18 ± 0.57	2.33 ± 1.90	<0.001
CPR (Z-Score)	0.23 ± 1.00	-2.35 ± 0.99	<0.001
UtA-PI (Z-score)	-0.64 ± 1.25	2.01 ± 2.09	<0.001
Perinatal Outcome			
Gestational age at delivery (weeks)	39.87 ± 1.81	34.29 ± 3.38	<0.001
Birth weight (grams)	3334 ± 536	1501 ± 556	<0.001
Birth-weight centile	55 ± 24	0 ± 1	<0.001
Pre-eclampsia	0	4 (26.7)	<0.001
1 min APGAR score <=7.0	0	3 (20)	<0.001
UA or UV pH at delivery <= 7.15	3 (13.6)	0 (0)	<0.001
Stillbirth	0	0	-
Fetal distress	2 (9.1)	2 (13.3)	0.683
Days in NCIU	0 ± 0	25 ± 22	<0.001
Neonatal morbidity	0 (0)	8 (53.3)	<0.001
Neonatal mortatility	0 (0)	1 (6.7)	<0.001

Data are given as mean ± SD or n (%). *Student's t-test for independent samples or Pearson χ^2 test. IUGR, intrauterine growth restriction; UA, umbilical artery; UV, umbilical vein; NCIU, neonatal intensive care unit; UtA, uterine artery; MCA, middle cerebral artery; CPR, cerebroplacental ratio; IFI, isthmic flow index; PI, pulsatility index;

Table 2. Model-based parameters estimated for all the fetal population

Model-based factors	*Control (n = 22)*	*IUGR (n=15)*	*p**
K_{RcorA} *(coronary arteries resistance)*	1.11 ± 0.21	0.88 ± 0.24	0.005
K_{rAo} *(aorta's radius)*	1.02 ± 0.09	0.99 ± 0.16	0.536
K_{Cao} *(aorta compliance)*	2.60 ± 0.93	2.74 ± 1.10	0.926
K_{rbA} *(brain arteries' radius)*	1.17 ± 0.20	1.08 ± 0.27	0.194
K_{CbA} *(brain arteries compliance)*	0.80 ± 0.60	0.94 ± 0.86	0.710
K_{Rb} (*brain resistance*)	1.36 ± 0.30	1.01 ± 0.31	0.003
K_{Cb} *(brain compliance)*	0.46 ± 0.16	0.64 ± 0.56	0.477
K_{Rrest} *(rest of peripheral resistance)*	0.74 ± 0.24	0.85 ± 0.30	0.252
K_{Crest} *(rest of peripheral compliance)*	1.09 ± 0.64	1.38 ± 0.69	0.130
K_{ruA} *(umbilical arteries' radius)*	1.05 ± 0.16	1.08 ± 0.21	0.805
K_{CuA} *(umbilical arteries' compliance)*	1.65 ± 0.60	1.84 ± 0.70	0.421
K_{Rplac} (*placental resistance*)	1.04 ± 0.35	3.75 ± 2.23	<0.001
K_{Cplac} *(placenta compliance)*	1.99 ± 0.99	3.79 ± 1.81	0.001

Data are given as mean ± SD. *Student's t-test or Mann-Whitney U test for normally and not normally distributed independent samples.

Table 3. Multiregression analysis between the Doppler and the model-based parameters

	K_{RcorA}	K_{Rb}	K_{Rplac}	K_{Cplac}	$\mathbf{R^2}$
IFI	0.349*	0.117	0.365	0.001	0.464**
MCA-PI	0.021	-0.216	0.569**	-0.382*	0.503**
UA-PI	0.004	-0.20	-0.41*	0.351*	0.555**
CPR	0.105	0.019	0.484**	-0.426**	0.669**
UtA-PI	-0.175	-0.014	-0.220	0.413*	0.402**

*p<0.05 and ** p<0.01

Table 4. Categories/subcategories of placental attributes (n=13) consistent with under perfusion in study population.

Categories of placental injury n (%)	***Subcategories of placental injury*** n (%)
Maternal vascular supply 10 (76.9)	Maldevelopment 2 (20)
	Obstruction 8 (80)
	Loss of integrity 0 (0)
Fetal vascular supply 3 (23.1)	Maldevelopment 0 (0)
	Obstruction 1 (33.3)
	Loss of integrity 2 (66.7)

Table 5. Doppler parameters before delivery and model-based parameters for the fetal population classified to have or not an adverse perinatal outcome

Feto-placental ultrasound	*Non-adverse outcome (n = 26)*	*Adverse outcome (n=11)*	*p**
AoI-PI (Z-Score)	2.31 ± 9.23	18.99 ± 33.55	0.023
IFI (Z-Score)	-0.38 ± 3.92	-5.75 ± 3.92	0.006
MCA-PI (Z-score)	-0.05 ± 1.06	-1.07 ± 1.29	0.016
UA-PI (Z-score)	0.18 ± 1.20	2.41 ± 1.07	<0.001
CPR (Z-Score)	-0.30 ± 1.33	-2.04 ± 1.61	0.002
UtA-PI (Z-score)	-0.05 ± 1.58	1.44 ± 2.69	0.047
Model-based parameters			
K_{RcorA} (coronary arteries resistance)	1.08 ± 0.21	0.87 ± 0.26	0.015
K_{Rb} (brain resistance)	1.33 ± 0.33	0.96 ± 0.20	0.003
K_{Rplac} (placental resistance)	1.39 ± 0.92	3.92 ± 2.60	0.001
K_{Cplac} (placental compliance)	2.32 ± 1.15	3.65 ± 2.21	0.022

Data are given as mean ± SD. * Student's t-test or Mann-Whitney U test for normally and not normally distributed independent samples. UA, umbilical artery; UtA, uterine artery; MCA, middle cerebral artery; CPR, cerebroplacental ratio; AoI, aortic isthmus; IFI, isthmic flow index; PI, pulsatility index.

Table 6. Accuracy, sensitivity and specificity results of the logistic regression analysis for detecting adverse perinatal outcome.

	Accuracy	*Sensitivity*	*Specificity*
Doppler set	88.6%	72.7%	95.8%
GA	89.2%	81.8%	92.3%
Doppler set + GA	91.4%	81.8%	95.8%
Doppler set + Model set	94.3%	90.9%	95.8%
GA + Model set	94.6%	90.9%	96.2%
Doppler set + GA+ Model set	97.1%	90.9%	100%

GA, gestational age at birth; Doppler parameter set includes: UA-PI, MCA-PI, CPR and UtA-PI, all in Z-scores. Model-based parameter set includes: K_{RcorA}, K_{Rb}, K_{Rplac} and K_{Cplac}.

FIGURE LEGENDS

Figure 1. A schematic representation of the lumped model of the fetal circulation composed of 19 arterial segments (black lines), 12 vascular beds (boxes) and 2 blood-flow inputs. UB: upper body; B: brain; L: lung; K: kidney; LB: lower body; P: placenta; QpA: pulmonary artery inflow; QAo: aortic inflow.

Figure 2. Block diagram of the patient-specific fitting algorithm.

Figure 3. (a)-(f) Left: Doppler recordings from (a) aortic isthmus (AoI), (c) middle cerebral artery (MCA), and (e) umbilical artery (UA) for a control fetus; Right: comparison between estimated (solid line) and measured Doppler velocity waveforms (dashed line) in the (b) AoI, (d) MCA and (f) UA for a control fetus. (g)-(l) Left: Doppler recordings from (g) AoI, (i) MCA and (k) UA for a IUGR fetus; Right: comparison between estimated (solid line) and measured Doppler velocity waveforms (dashed line) in the (h) AoI, (j) MCA and (l) UA for a IUGR fetus.

Figure 4. Model-based parameters estimated with the model for the 13 placentas histologically evaluated: (a) coronary arteries resistance (K_{RcorA}), (b) brain resistance (K_{Rb}), (c) Placental resistance ($1/K_{Rplac}$) and (d) placental compliance ($1/K_{Cplac}$). MUP: maternal under-perfussion; FUP: fetal under-perfussion

Figure 5. Model-based parameters estimated with the model for the three groups: controls, IUGR and fetuses with adverse perinatal outcome (APO): (a) coronary arteries resistance (K_{RcorA}), (b) brain resistance (K_{Rb}), (c) placental resistance (K_{Rplac}) and (d)

placental compliance (K_{Cplac}). APO: adverse perinatal outcome. *p value < 0.05 compared with the control group; **p value < 0.01 compared with the control group.

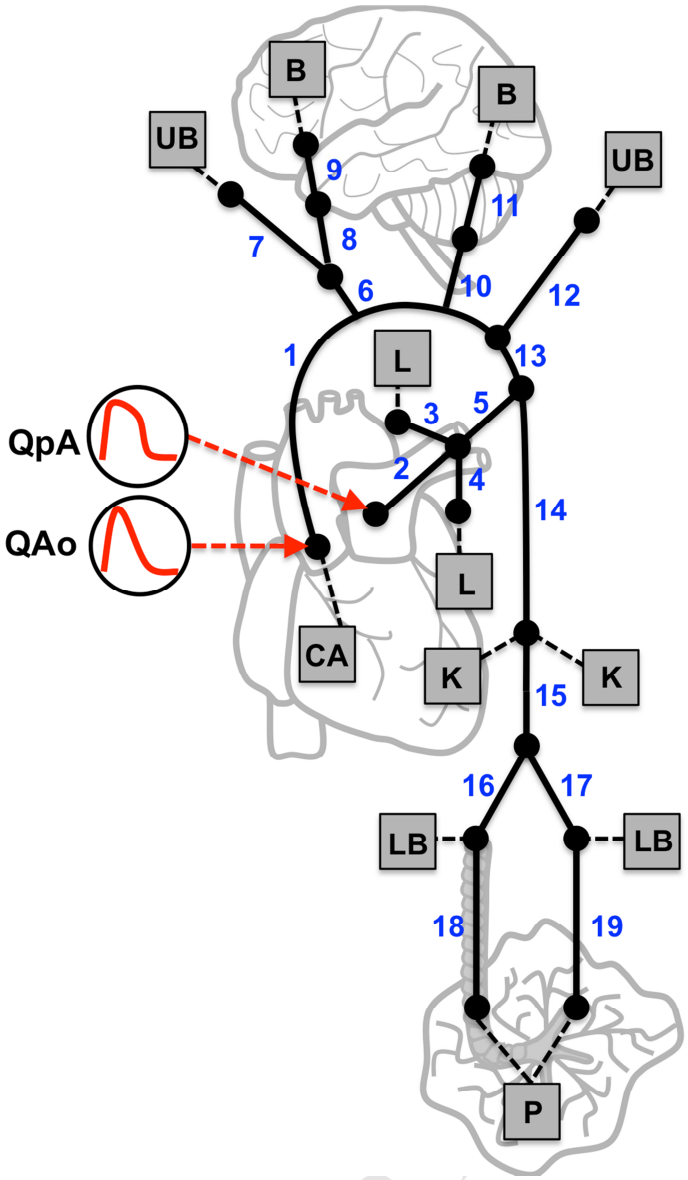

1. Ascending Aorta
2. Main Pulmonary artery
3. R. Pulmonary Artery
4. L. Pulmonary Artery
5. Ductus Arteriosus
6. Brachiocephalic Trunk
7. R. Subclavian Artery
8. R. Common Carotid Artery
9. R. Internal Carotid Artery
10. L. Common Carotid Artery
11. L. Internal Carotid Artery
12. L. Subclavian Artery
13. Aortic Isthmus
14. Thoracic Aorta
15. Abdominal Aorta
16. R. Illiac Artery
17. L. Illiac Artery
18. R. Umbilical Artery
19. L. Umbilical Artery

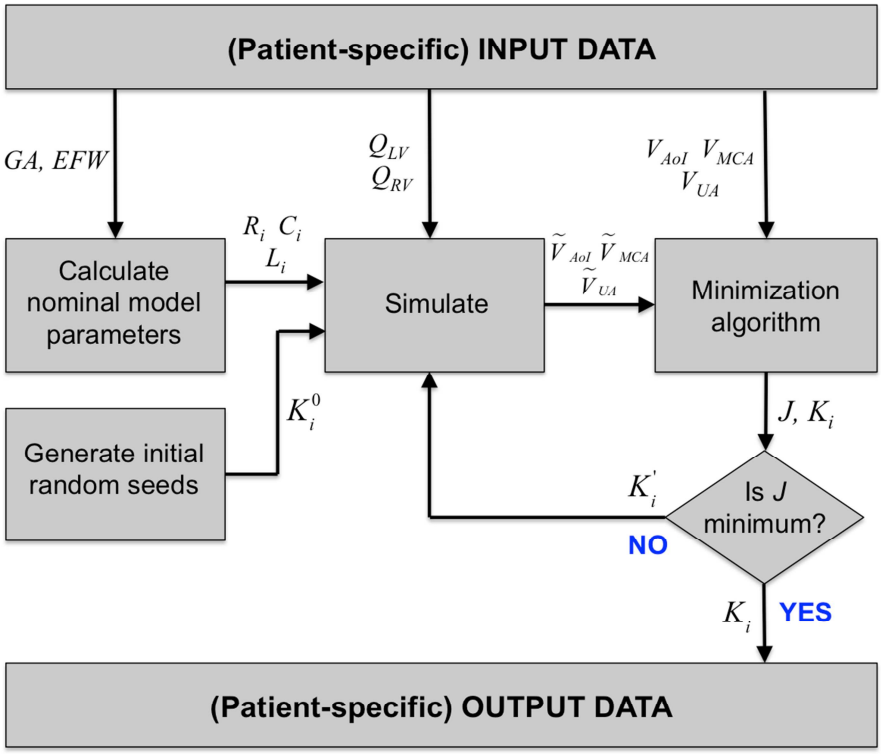

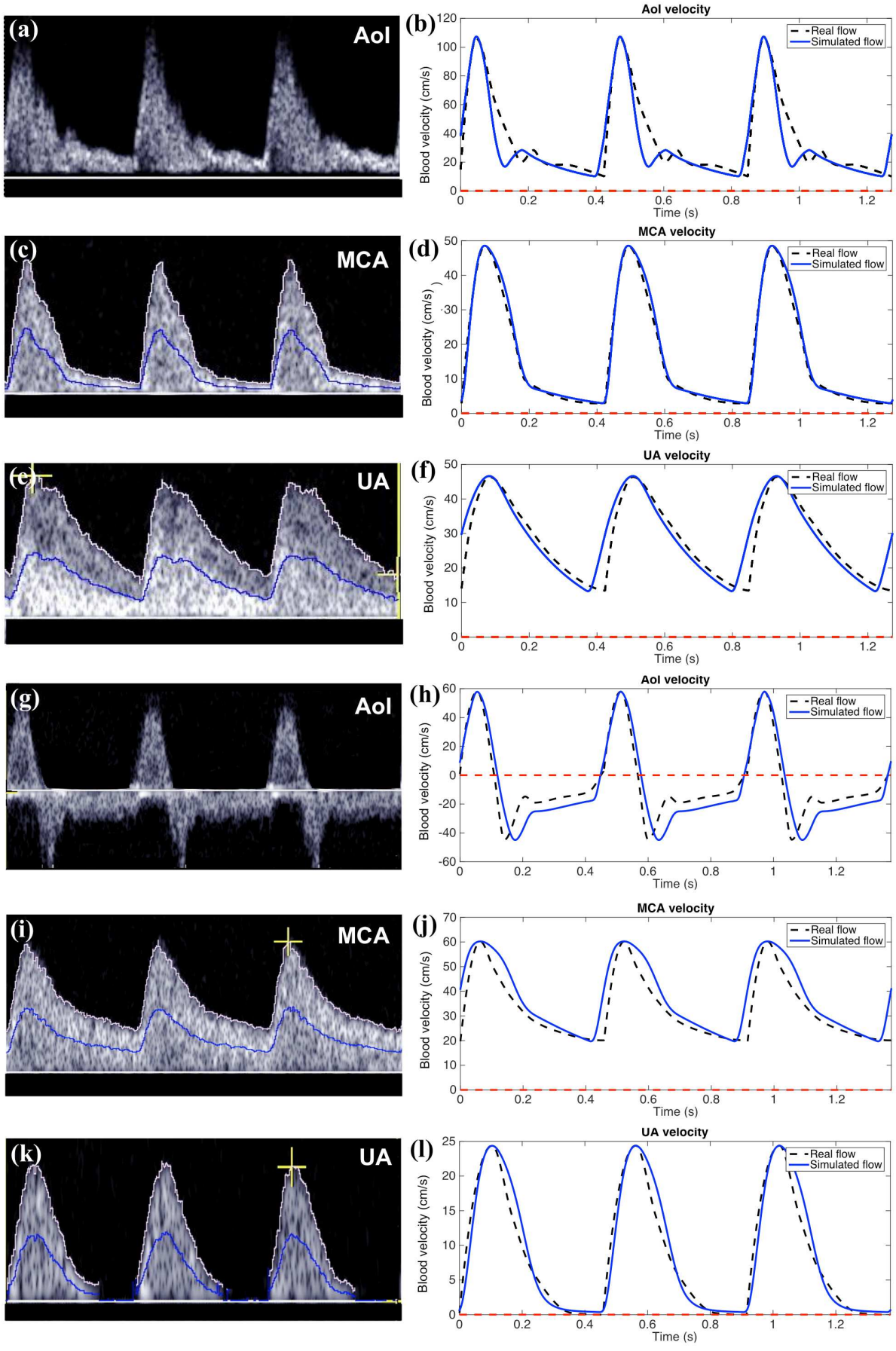
(a)
AoI
(b)
AoI velocity
Real flow
Simulated flow
Blood velocity (cm/s)
Time (s)
(c)
MCA
(d)
MCA velocity
Real flow
Simulated flow
Blood velocity (cm/s)
Time (s)
(e)
UA
(f)
UA velocity
Real flow
Simulated flow
Blood velocity (cm/s)
Time (s)
(g)
AoI
(h)
AoI velocity
Real flow
Simulated flow
Blood velocity (cm/s)
Time (s)
(i)
MCA
(j)
MCA velocity
Real flow
Simulated flow
Blood velocity (cm/s)
Time (s)
(k)
UA
(l)
UA velocity
Real flow
Simulated flow
Blood velocity (cm/s)
Time (s)

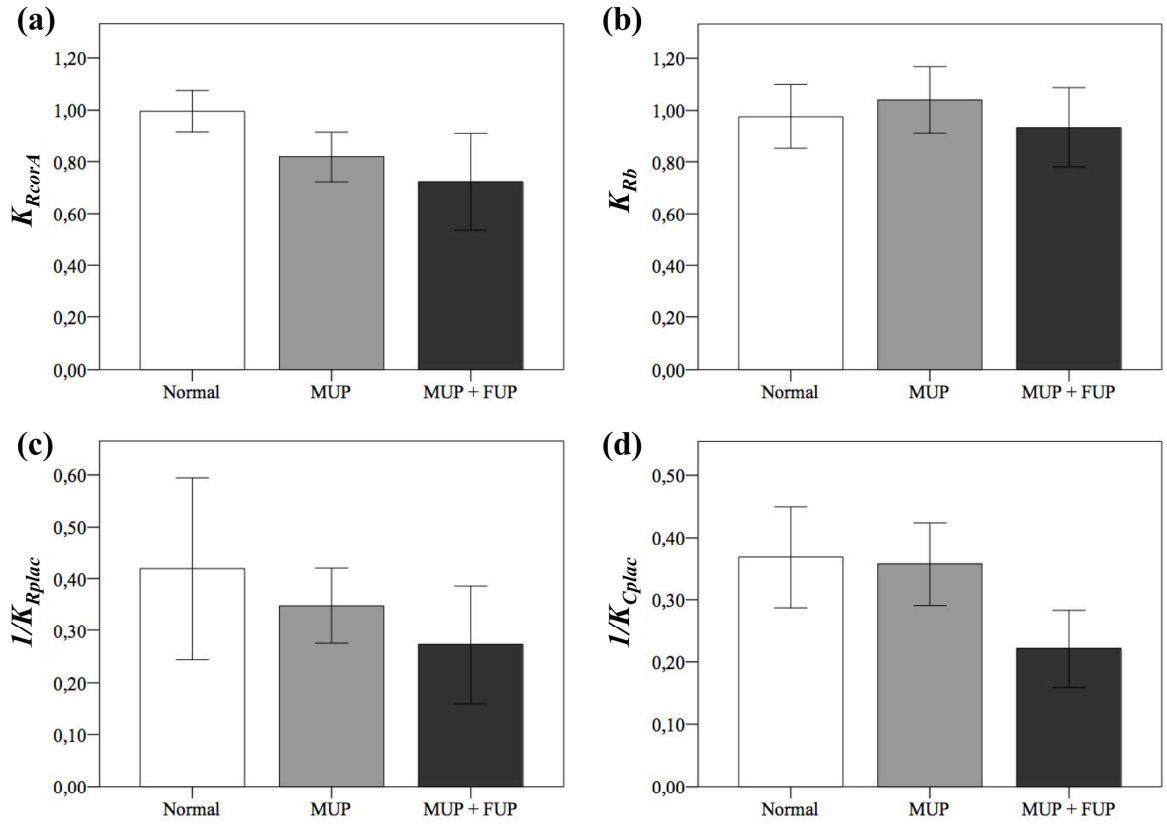

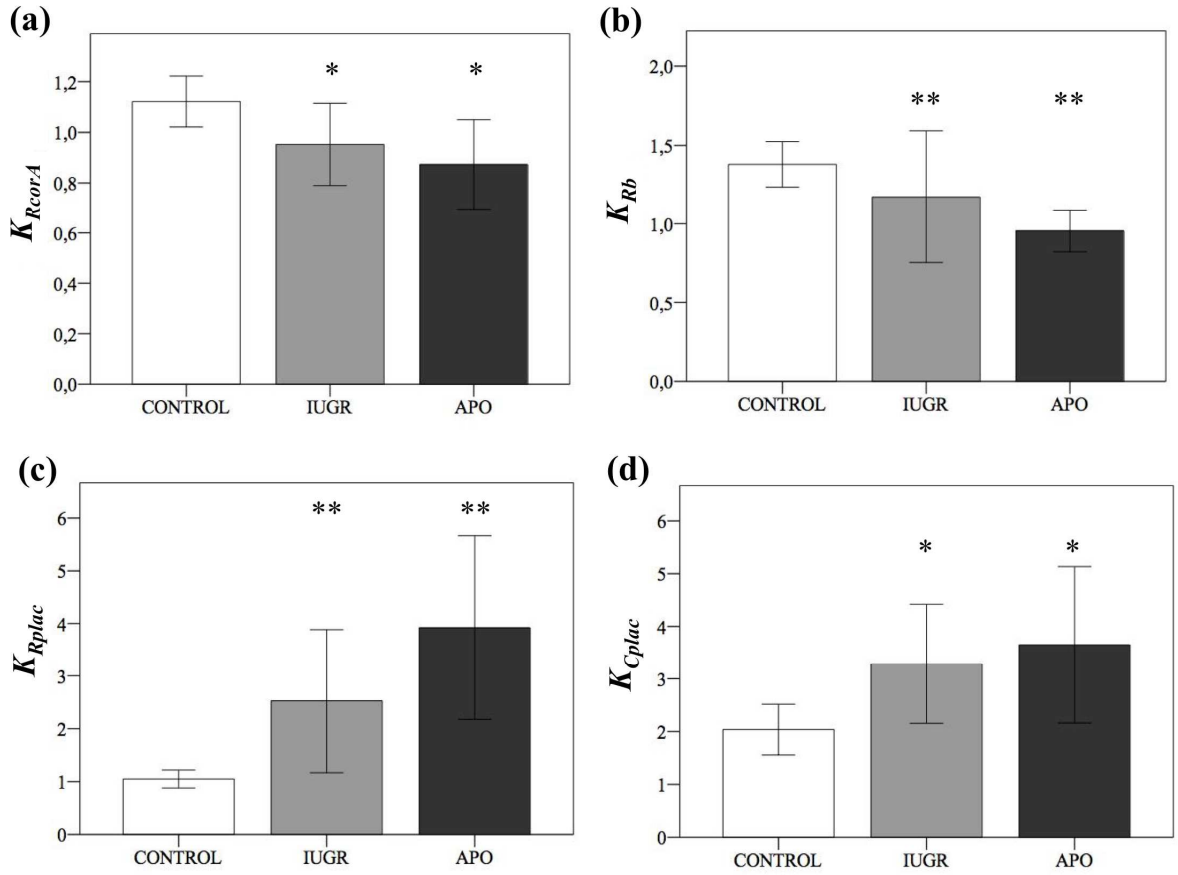

HIGHLIGHTS

1. We implemented a patient-specific model of the fetal circulation.
2. We estimated the vascular and placental properties of 22 controls and 15 IUGR fetuses.
3. Model parameters were differently associated to the different Doppler indices.
4. Model parameters improved the detection of adverse outcome in IUGR.

Supplementary methods

1. Ultrasonographic evaluation.

Estimated fetal weight (EFW) was calculated from the biparietal diameter, head and abdominal circumference, and femur length using the Hadlock formula [1]. Umbilical artery (UA) was evaluated in a free loop of the umbilical cord. Middle cerebral artery (MCA) was measured in a transverse view of the fetal skull at the level of its origin from the circle of Willis [2]. For uterine artery (UtA) assessment, the ultrasound probe was placed on the lower quadrant of the abdomen, angled medially, and color Doppler imaging was used to identify the UtA at the apparent crossover with the external iliac artery. Mean UtA-PI was calculated as the average PI of the right and left arteries. Cerebroplacental ratio was calculated by dividing MCA and UA PI. PI was calculated as: (systolic – diastolic) velocities divided by time-averaged maximum velocity. Aortic isthmus (AoI) flow velocity was recorded either in a sagittal view of the fetal thorax with a clear visualization of the aortic arch or in a cross section of the fetal thorax at the level of the 3-vessel and trachea view. The AoI-PI and flow index (IFI) were measured. The IFI was calculated as: (systolic + diastolic)/systolic velocity integrals. Left ventricular (LV) outflow was imaged in an apical or basal 5-chamber view of the heart at the aortic outflow tract, and right ventricular (RV) outflow was obtained in a RV outflow tract view. Peak systolic velocities of both LV and RV outflow, ejection time and heart rate were measured. Doppler recordings were done in absence of fetal movements and, when required, with voluntary suspended maternal breathing. The angle of insonation between the vessel and the Doppler beam was kept as close as possible to 0º and always below 30º. Doppler parameters were obtained form three or more successive waveforms in each vessel. Finally, diameters of the aortic and

pulmonary artery valves were measured in frozen real-time images during systole by the leading edge-to-edge method [3].

2. Placental evaluation

Among maternal vascular supply disruptions, specific vascular alterations qualifying for maternal vascular maldevelopment were: superficial implantation/decidual arteriopathy (acute atherosis and mural hypertrophy [mean wall diameter>30% of overall vessel diameter of arterioles in the decidua parietalis]), undergrowth/distal villous hypoplasia (decrease in the number and modal diameter of distal villi at the center of the lobule after adjustment for plane of section and gestational age, in the lower 75% of a full-thickness section), excessive intervillous fibrin (basal layer of fibrinoid material involving > 30% of the placental maternal surface) and migration disorders. Specific vascular alterations qualifying for maternal vascular obstruction were: syncytial knots involving terminal villi (affecting >50% of the terminal villi), villous agglutination (>50%), intervillous fibrin deposition (eccentric aggregates on intervillous fibrin on proximal and distal villi affecting >50% of the villi) and villous infarcts (>30% of villous loss). Specific vascular alterations qualifying for maternal vascular loss of integrity were: arterial rupture (abruption placenta), venous rupture (acute chronic marginal abruption).

Among fetal vascular supply disruptions, lesions qualifying for maldevelopment were: chorioangioma, chorioangiosis and distal villous immaturity. Lesions qualifying for obstruction were considered those secondary to vascular thrombo-occlusive disease (thrombosis of chorionic plate and stem villous channels and villous avascularity affecting large groups).

3. Patient-specific input data

Patient-specific blood velocity waveforms from right and left output tracks (V_{RV} and V_{LV}), MCA (V_{MCA}), AoI (V_{AoI}) and UA (V_{UA}) were obtained by manual delineation of the envelope of the Doppler blood velocity profiles. The corresponding blood-flows: Q_{LV}, Q_{RV}, Q_{MCA}, Q_{AoI} and Q_{UA} were calculated considering the shape (parabolic or flat) of the velocity profiles. This property is described by the Womersley number (W), a dimensionless parameter calculated as: $W = D\sqrt{f\pi/2\eta}$, where D is the vessel diameter, η is the blood viscosity and f the frequency given by the heart rate. Then, blood-flows were calculated accordingly as: $Q_i = V_i \cdot \pi \cdot (D/2)^2 \cdot k$, where k is a factor that depends on the Womersley number as described by Ponzini et al [4].

The GA and the EFW were used to calculate the different electrical components of the equivalent circuit. Firstly, arterial radius, length and thickness were calculated using the equations described in the Table S1, which depends on the GA. Then, in order to describe the changes in the vessel dimensions as a function of EFW, the dimensions of all the arterial segments were scaled according to the following equation: $Y_i = Y_0 \left(EFW/W_0\right)^{0.33}$ as described by Pennati et al [5], where W_0 is the reference EFW calculated using the following relationship between the GA and W_0: $log_{10}(W_0) = 0.2508 + 0.1458 \cdot GA - 0.0016 \cdot GA^2$ [6], with GA in weeks. Blood viscosity was calculated as: $\mu = (1.15 + 0.075 \times GA)/100$ [7], with the GA in weeks. The variation of the arterial Young's moduli of each arterial segment with the GA was considered as described by van den Wijngaard et al [7]. Regarding the vascular bed components, compliances were scaled to their values at each corresponding GA, following the expression reported by van Gemert et al [8]. Resistances were scaled to obtain a mean blood pressure (MBP) adequate for each GA and calculated as: *MBP (mmHg) = 0.87*GA+10.33* [9].

Then, vascular bed resistances and compliances were also scaled to take into account the EFW of the fetus, following the equations described in [5]: $R_p = R_{p0} \cdot (EFW/W_0)^b$ and $C_p = C_{p0} \cdot (EFW/W_0)^b$ respectively, where b is the scaling factor (see Table S2), and R_{p0} and C_{p0} were the vascular bed resistance and compliance respectively, calculated for the specific GA.

4. Patient-specific fitting

The input of the model was defined as the set of the initial values of all the electrical components, calculated for each fetus as described in the previous section, and the two patient-specific blood-flow inputs: Q_{RV} and Q_{LV}. The output was defined as the model-based blood velocities in the AoI ($\widetilde{V}_{AoI}$), MCA ($\widetilde{V}_{MCA}$) and UA ($\widetilde{V}_{UA}$). In order to fit the model-based blood velocities to the measured ones, some of the model parameters needed to be estimated, and therefore, an optimization algorithm was defined.

Since the number of total parameters in the model is to large, in order to obtain an efficient solution of the patient-specific modeling, a reduction in the number of model parameters to be estimated was necessary and, therefore, a subset of only few parameters was defined. The selection criteria were: (1) those parameters that are relevant in the adaptation mechanisms of IUGR fetuses and (2) those parameters that when varied, the output of the model varied significantly also. The factors (K_i) indicating the variation of the model parameters with respect to their nominal values were estimated ($K_i = I/I_0$). Therefore, a set of 13 factors (K) were defined: $K = \{K_{RcorA}, K_{rAo}, K_{CAo}, K_{rbA}, K_{CbA}, K_{Rb}, K_{Cb}, K_{Rrest}, K_{Crest}, K_{ruA}, K_{CuA}, K_{Rplac}, K_{Cplac}\}$ (*RcorA*: coronary arteries resistance, *rAo*: radius of the whole aorta (aortic arch + ascending, thoracic and abdominal aorta), *CAo*: compliance of the aorta, *rbA*: radius of the brain arteries, *CbA*: compliance of the brain arteries, *Rb*: brain's resistance, *Cb*: brain's compliance, *Rrest*:

the resistance of the rest of vascular beds (lungs, upper body, kidneys and lower body), *Crest*: compliance of the rest of vascular beds (lungs, upper body, kidneys and lower body), *ruA*: radius of the umbilical artery, *CuA*: compliance of the umbilical artery, *Rplac*: placenta's resistance and *Cplac*: placenta's compliance.

To estimate the variation factors of the model parameters we used a constrained nonlinear optimization algorithm minimizing the normalized relative root mean square error (NRMSE) between the model-based (denoted by ~) and measured velocity waveforms. To ensure that the model estimates correctly both systolic and diastolic extreme values of the blood velocities waveforms, we also included in the minimization objective function the relative error between model-based and measured values of each of these. Therefore, the objective function J was defined as the sum of individual relative errors as:

$$J = \sum_{i=AoI,MCA,UA} \left[\frac{\sqrt{\frac{1}{N}\sum_{t=1}^{N}\left(\tilde{V}_i(t) - V_i(t)\right)^2}}{max(V_i(t)) - min(V_i(t))} + \frac{\tilde{V}_i(t_{sys}) - V_i(t_{sys})}{V_i(t_{sys})} + \frac{\tilde{V}_i(t_{dias}) - V_i(t_{dias})}{V_i(t_{dias})} \right]$$

where i indicates one of the three places of the fetal circulation were blood velocity was measured: *AoI*, MCA or *UA*; N is the number of time points and t_{sys} and t_{dias} are the systolic and diastolic time points respectively. To do this, the model was initialized with the nominal model parameters that describe a normal fetus with same GA and EFW, and with an initial set of K_i factors. Then, the estimation problem consisted on searching the set of factors ($K = \{K_i\}$) that minimizes J. The initial set of factors K was randomly defined within a physiological range. Then, to avoid local minim solutions, the optimization procedure was repeated several times with different initial K, and we finally chose the K with the minimum J value.

Table S1. Equations describing the dimensions and Young's moduli (E) of the different arterial segments of the fetal circulation lumped model.

Arterial Segment	Length (mm)	Diameter (mm)	E (dyn/cm^2)
Ascending Aorta	$-8.61 + 0.88 \cdot t$	$-2.10 + 0.27 \cdot t$	$1.57 \cdot (3.8 \cdot 10^2\ t^2 + 4.7 \cdot 10^3 \cdot t + 1.5 \cdot 10^4)$
Aortic isthmus	$-2.15 + 0.22 \cdot t$	$-1.86 + 0.19 \cdot t$	$1.57 \cdot (3.8 \cdot 10^2\ t^2 + 4.7 \cdot 10^3 \cdot t + 1.5 \cdot 10^4)$
Thoracic Aorta	$-19.65 + 2.05 \cdot t$	$-2.38 + 0.24 \cdot t$	$1.89 \cdot (3.8 \cdot 10^2\ t^2 + 4.7 \cdot 10^3 \cdot t + 1.5 \cdot 10^4)$
Abdominal Aorta	$-14.59 + 1.52 \cdot t$	$-2.07 + 0.21 \cdot t$	$4.19 \cdot (3.8 \cdot 10^2\ t^2 + 4.7 \cdot 10^3 \cdot t + 1.5 \cdot 10^4)$
Ductus Arteriosus	$-2.41 + 0.31 \cdot t$	$-2.09 + 0.21 \cdot t$	$2.83 \cdot (3.8 \cdot 10^2\ t^2 + 4.7 \cdot 10^3 \cdot t + 1.5 \cdot 10^4)$
Main pulmonary artery	$-5.60 + 0.57 \cdot t$	$-2.77 + 0.30 \cdot t$	$1.57 \cdot (3.8 \cdot 10^2\ t^2 + 4.7 \cdot 10^3 \cdot t + 1.5 \cdot 10^4)$
R. pulmonary artery	$-4.00 + 0.41 \cdot t$	$-1.71 + 0.18 \cdot t$	$1.57 \cdot (3.8 \cdot 10^2\ t^2 + 4.7 \cdot 10^3 \cdot t + 1.5 \cdot 10^4)$
L. pulmonary artery	$-4.00 + 0.41 \cdot t$	$-1.95 + 0.19 \cdot t$	$1.57 \cdot (3.8 \cdot 10^2\ t^2 + 4.7 \cdot 10^3 \cdot t + 1.5 \cdot 10^4)$
Brachiocephalic Trunk	$-1.06 + 0.29 \cdot t$	$-1.78 + 0.18 \cdot t$	$1.89 \cdot (3.8 \cdot 10^2\ t^2 + 4.7 \cdot 10^3 \cdot t + 1.5 \cdot 10^4)$
L. subclavian artery	$-2.15 + 0.43 \cdot t$	$-1.22 + 0.12 \cdot t$	$2.83 \cdot (3.8 \cdot 10^2\ t^2 + 4.7 \cdot 10^3 \cdot t + 1.5 \cdot 10^4)$
R. subclavian artery	$-2.15 + 0.43 \cdot t$	$-1.22 + 0.12 \cdot t$	$2.83 \cdot (3.8 \cdot 10^2\ t^2 + 4.7 \cdot 10^3 \cdot t + 1.5 \cdot 10^4)$
L. Common Carotid artery	$-9.69 + 1.59 \cdot t$	$-1.52 + 0.14 \cdot t$	$2.83 \cdot (3.8 \cdot 10^2\ t^2 + 4.7 \cdot 10^3 \cdot t + 1.5 \cdot 10^4)$
R. Common Carotid artery	$-8.25 + 1.36 \cdot t$	$-1.52 + 0.14 \cdot t$	$2.83 \cdot (3.8 \cdot 10^2\ t^2 + 4.7 \cdot 10^3 \cdot t + 1.5 \cdot 10^4)$
L. Internal Carotid artery	$-8.25 + 1.36 \cdot t$	$-1.22 + 0.11 \cdot t$	$4.61 \cdot (3.8 \cdot 10^2\ t^2 + 4.7 \cdot 10^3 \cdot t + 1.5 \cdot 10^4)$
R. Internal Carotid artery	$-8.25 + 1.36 \cdot t$	$-1.22 + 0.11 \cdot t$	$4.61 \cdot (3.8 \cdot 10^2\ t^2 + 4.7 \cdot 10^3 \cdot t + 1.5 \cdot 10^4)$
L. Common Illiac artery	$-3.11 + 0.55 \cdot t$	$1.28 - 0.09 \cdot t + 0.004 \cdot t^2$	$6.39 \cdot (3.8 \cdot 10^2\ t^2 + 4.7 \cdot 10^3 \cdot t + 1.5 \cdot 10^4)$
R. Common Illiac artery	$-3.59 + 0.59 \cdot t$	$1.39 - 0.11 \cdot t + 0.004 \cdot t^2$	$6.39 \cdot (3.8 \cdot 10^2\ t^2 + 4.7 \cdot 10^3 \cdot t + 1.5 \cdot 10^4)$
L. Umbilical artery	$60 \cdot t/40$	$0.0082 + 0.0094 \cdot t$	$12.67 \cdot (3.8 \cdot 10^2\ t^2 + 4.7 \cdot 10^3 \cdot t + 1.5 \cdot 10^4)$
R. Umbilical artery	$60 \cdot t/40$	$0.0082 + 0.0094 \cdot t$	$12.67 \cdot (3.8 \cdot 10^2\ t^2 + 4.7 \cdot 10^3 \cdot t + 1.5 \cdot 10^4)$

t represents the gestational age in weeks.

Table S2. Exponents "b" of the allometric equations for scaling vascular bed resistances and compliances

Scaling factors (b)	*Vascular bed resistance (R_p)*	*Vascular bed compliance (C_p)*
Brain	-1.10	1.47
Upper body	-1.00	1.33
Lungs	-1.20	1.60
Lower body	-1.00	1.33
Kidneys	-1.00	1.33
Placenta	-1.00	1.33

REFERENCES

[1] Hadlock FP, Harrist RB, Shah YP, King DE, Park SK, Sharman RS. Estimating fetal age using multiple parameters: a prospective evaluation in a racially mixed population. Am J Obs Gynecol 1987;156:955–7.

[2] Arduini D, Rizzo G. Normal values of Pulsatility Index from fetal vessels: a cross-sectional study on 1556 healthy fetuses. J Perinat Med 1990;18:165–72.

[3] Schneider C, McCrindle BW, Carvalho JS, Hornberger LK, McCarthy KP, Daubeney PEF. Development of Z-scores for fetal cardiac dimensions from echocardiography. Ultrasound Obstet Gynecol 2005;26:599–605. doi:10.1002/uog.2597.

[4] Ponzini R, Vergara C, Rizzo G, Veneziani A, Roghi A, Vanzulli A, et al. Womersley number-based estimates of blood flow rate in Doppler analysis: in vivo validation by means of phase-contrast MRI. IEEE Trans Biomed Eng 2010;57:1807–15. doi:10.1109/tbme.2010.2046484.

[5] Pennati G, Fumero R. Scaling approach to study the changes through the gestation of human fetal cardiac and circulatory behaviors. Ann Biomed Eng 2000;28:442–52.

[6] Gallivan S, Robson SC, Chang TC, Vaughan J, Spencer JA. An investigation of fetal growth using serial ultrasound data. Ultrasound Obs Gynecol 1993;3:109–14. doi:10.1046/j.1469-0705.1993.03020109.x.

[7] Van den Wijngaard JPHM, Westerhof BE, Faber DJ, Ramsay MM, Westerhof N, van Gemert MJC. Abnormal arterial flows by a distributed model of the fetal circulation. Am J Physiol Regul Integr Comp Physiol 2006;291:R1222–33. doi:10.1152/ajpregu.00212.2006.

[8] Van Gemert MJC, Sterenborg HJ, C MJCVG. Haemodynamic Model of Twin-Twin Transfusion Syndrome. Placenta 1998;19:195–208.

[9] Struijk PC, Mathews VJ, Loupas T, Stewart PA, Clark EB, Steegers EA, et al. Blood pressure estimation in the human fetal descending aorta. Ultrasound Obs Gynecol 2008;32:673–81. doi:10.1002/uog.6137.